ELECTRONIC SUPPORTING INFORMATION

Engineering Surface Wettability of Ceramic Carbon Electrode for Improved Hydrogen Evolution Performance of Molybdenum Sulfide Electrocatalyst

Yun-Chen Tsai[1], Truong-Giang Vo[1], Chia-Ying Chiang[1]*

[1] Department of Chemical Engineering, National Taiwan University of Science and Technology, Taipei-106, Taiwan

*Corresponding Authors:

Prof. **Chia-Ying Chiang**

Phone: +886-2-2737-6641
Fax: +886-2-2737-6644
E-mail: cychiang@mail.ntust.edu.tw

Morphology and crystal structure characterization

Surface hydrophilicity of CCE substrate were determined by using water contact angle meter (CAM120, Creating Nano Technologies Inc.). Fourier-transform infrared spectroscopy (FT-IR) spectrums were recorded in the range of 4000–400 cm^{-1} with a FTS-3500 spectrometer (Bio-Rad, USA). Field-emission scanning electron microscope (FE-SEM; JSM-6500F) with an energy dispersive X-ray (EDX) was used for showing the morphology of samples. X-ray photoelectron spectroscopy (XPS) (VG ESCA Scientific Theta Probe & VG Scientific ESCALAB 250) was used for surface element composition analysis. The MoS_x crystallinity was measured by X-ray diffractometer (Bruker, D2-Advance X-ray diffractometer, Cu Kα, λ = 1.5406 Å). Scanning electron microscopy (SEM) (Hitachi, SU8220). Prior to the TEM measurements, samples were scratched from CCE substrate and was dispersed in ethanol solution using ultrasound, then the obtained solution was dropped onto a copper grid. All bright field (BF) and dark field (DF) scanning transmission electron microscopy (STEM) were collected in a Hitachi SU8200 SEM instrument at an accelerating voltage of 30 kV. For STEM-EDX mapping measurements were recorded using the TE detector for signal and the FlatQuad detector for spectral acquisition. Raman measurements were performed on a confocal Raman microscope system (MRID, Protrustech, Taiwan). A solid-state laser operating at $\lambda = 532$ nm was used as the excitation source. To prevent degradation, the exposure time was set at 3 seconds with 10 accumulations. An objective lens 50× was used and the measurement was carried out at room temperature and under dark conditions. Before the measurement, the Raman band of a silicon wafer at 520 cm^{-1} was used as the standard reference to calibrate the spectrometer.

Electrochemical performance evaluation

Hydrogen evolution reaction (HER) activities were evaluated via linear sweep voltammetry (LSV) in 0.5 M H_2SO_4 solution (pH 0.5) at a scan rate of 5 mV/s. All LSV measurements were performed on at least three different samples, and representative data are reported. Cyclic voltammogram (CV) were taken several cycles to remove away the surface contaminates before any measurement. The working electrode was either a modified CCE with or without depositing MoS_x

(exposed area = 1.5 cm^2). Additionally, the CCEs modified with materials was measured in 5 mM $K_3[Fe(CN)_6]$ with 0.1 M KCl solution to obtain the CV curves and calculate for the electrochemically active surface area. The electrochemical impedance spectroscopy (EIS) was performed from 100 kHz to 100 mHz using an amplitude of 10 mV at a set potential of −0.25 V vs. RHE. The long-term stability photoanodes for oxygen evolution reaction was evaluated by chronoamperometry with a controlled potential at -0.25 V for several hours. The solution was gently stirred to circulate the electrolyte and remove bubbles from the film surface.

All the electrochemical measurements were conducted using an electrochemical workstation (Autolab PGSTAT302N, Netherlands). Standard three-electrode setup containing a Ag/AgCl (in 3 M KCl) as the reference, a Pt mesh (2.5 cm × 2.5 cm) as the counter, and the modified CCEs as working electrodes. All HER results were corrected for all ohmic (IR) losses throughout the system. To obtain the ohmic resistance, the electrochemical impedance spectroscopy (EIS) measurements were performed with frequency from 100 kHz to 0.1 Hz at an amplitude of 10 mV.

The electrochemical surface area (ESA) was estimated from the double-layer capacitance (C_{dl}) of the films. The C_{dl} was determined with a simple cyclic voltammetry (CV) method. The CV was conducted at various scan rates of 1, 5, 10, 20 mV/s. Then capacitive current was plotted against various scan rates, while the slope obtained was divided by two to obtain the C_{dl} value.

The Faradaic efficiency of the catalysts was determined by passing 10 mA/cm^{-2} of current density through the water electrolysis system and the hydrogen gas generated was determined by analyzing 400 μL of headspace samples via gas chromatography (YL6500GC, Young Lin Instrument Co., Korea) equipped with a thermal conductivity detector (TCD) and a stainless-steel molecular sieve 5A packed column (10 ft length). Argon with flow rate of 12 mL/min was used as the carrier gas. The Faradaic efficiency is then defined as the ratio of the measured amount of H_2 to that of the theoretical amount of H_2 (based on Faraday's law).

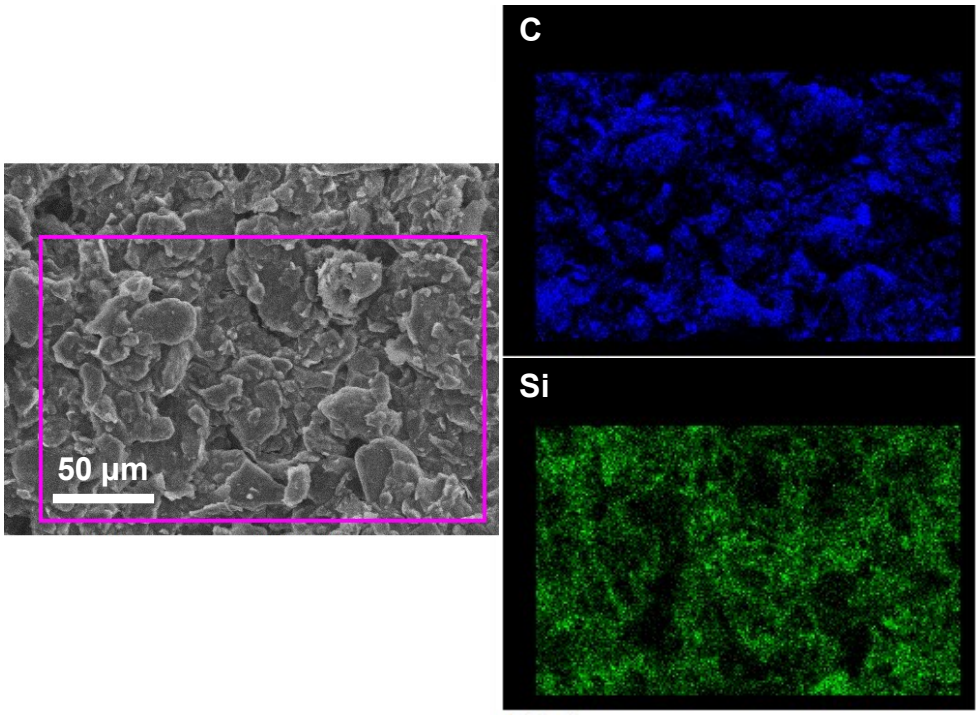

Figure S1 SEM images and EDS elemental mapping carbon and silicon for HI-CCE.

Table S1 Electrical properties of HO-CCE and HI-CCE

	Resistance (Ω)	Thickness (mm)	Electric conductivity (S/cm)	Resistivity (Ω.cm)
HO-CCE	0.357	~2.0	1.3	0.714
HI-CCE	0.053	~2.0	5.3	0.106

Electrochemically active surface area calculation

The electrochemically active surface area can be estimated from the peak current by using the Randle–Sevcik equation[1–3] $I_p = 2.69\times10^5 A D^{1/2} n^{3/2} v^{1/2} C$ where n is the number of electrons involved in the redox reaction, A is the surface area of the electrode (cm^2), D is the diffusion coefficient of the molecule in the bulk solution (6.67×10^{-6} cm^2 s^{-1} for ferricyanide), C is the concentration of the molecule in the bulk solution (M), and v is the scan rate (V s^{-1}).

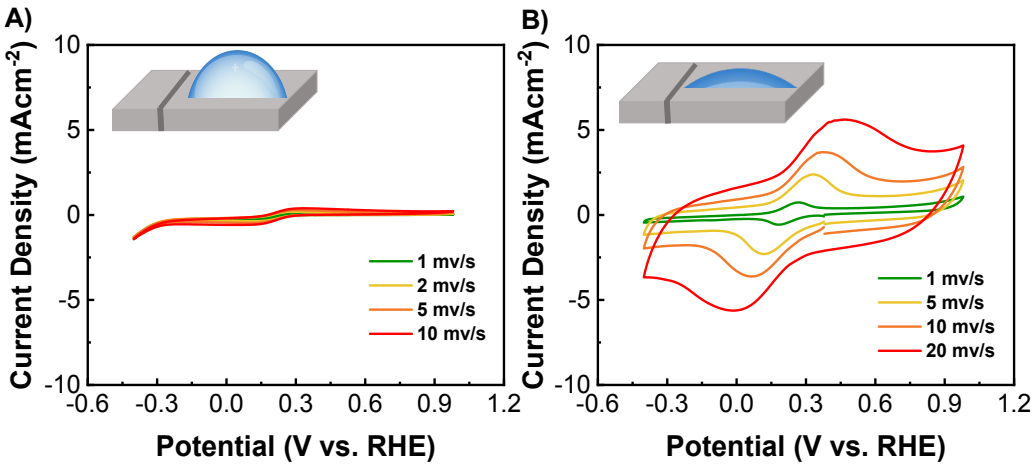

Figure S2 Cyclic voltammograms of HO-CCE (a, zoomed in inset) and HI-CCE (b) at different potential scanning rates from 1 to 10 mVs^{-1}.

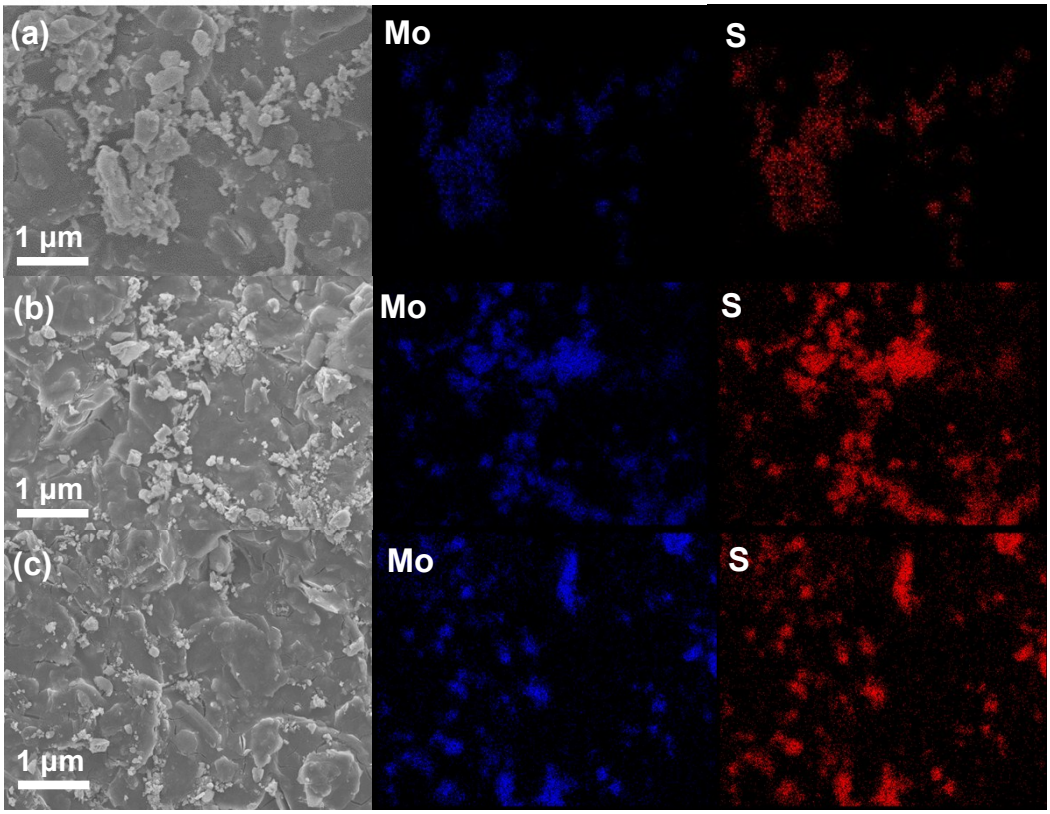

Figure S3 SEM images and element mapping (Mo, S) of HO-CCE/MoS_x (a), HI-CCE/MoS_x (b) and HI-CCE/MoS_x (DMF: H_2O) (c).

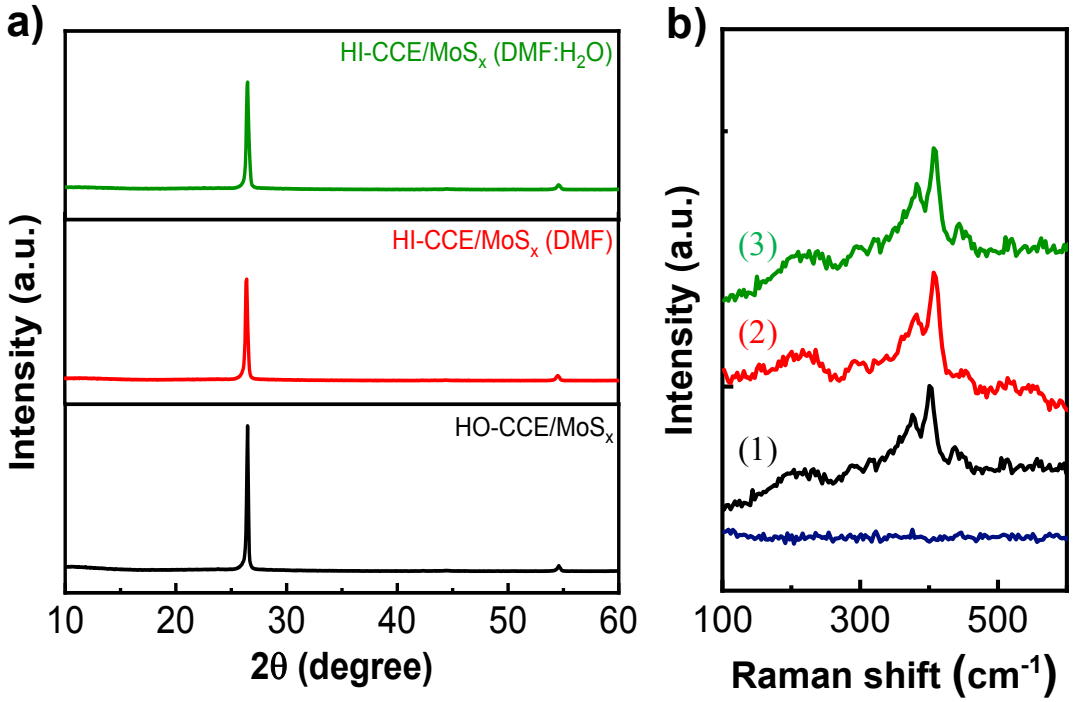

Figure S4 XRD patterns (a) and Raman spectra (b) of HO-CCE/MoS_x (1), HI-CCE/MoS_x (2) and HI-CCE/MoS_x (DMF: H_2O) (3).

To further obtain the details of morphology, TEM images of HI-CCE/MoS_x was taken. The bright-field and dark-field TEM images (**Fig. S5**) of HI-CCE/MoS_x confirms that the material is composed of irregularly shaped, agglomerated particles with most of them smaller than 50 nm in diameter (**Fig. S5**).

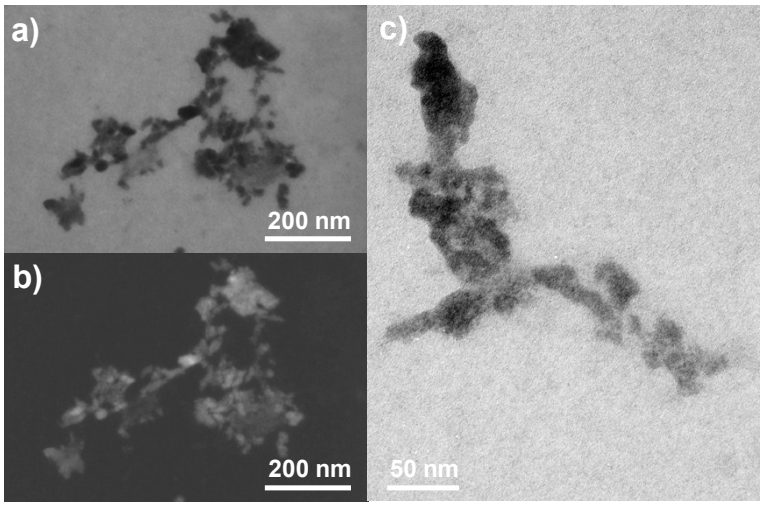

Figure S5 Dark field scanning TEM (DFSTEM) (a), bright field scanning TEM (BFSTEM) images (b) and high-maginification TEM images of HI-CCE/MoS_x (c)

The elemental composition analysis indicated an S/Mo ratio of 2.3 in this sample.

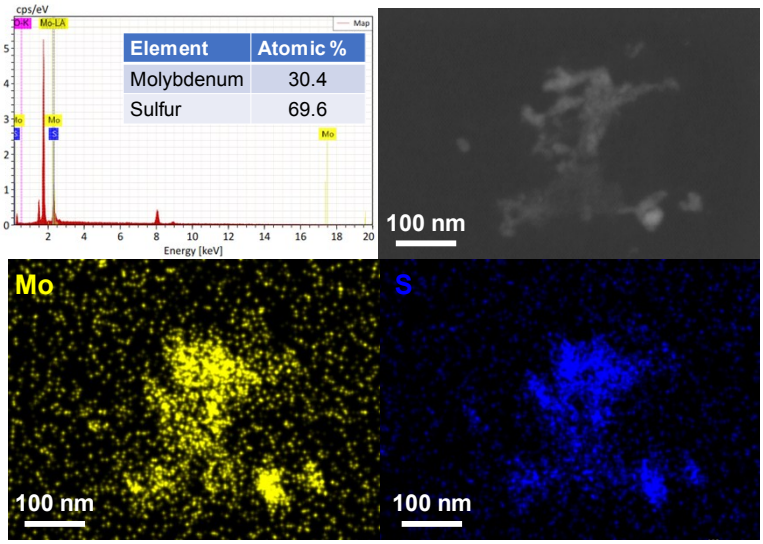

Figure S6 EDS specta of the HI-CCE/MoS_x (a). The dark field scanning TEM (DFSTEM) images and corresponding elemental mapping images of HI-CCE/MoS_x. indicationg the evenly distribution of Mo ad S.

Additional discussion related to using different counter electrode in evaluating HER activity

Researchers have recently raised concerns about the appropriateness of using Pt as counter electrode in evaluating HER activity. It is reported that Pt might be oxidized and dissolved under certain chemical or electrochemical circumstances, especially high potential and large current, and then might be electro-reduced onto the working electrode. Therefore, in order to validate the good HER activity in this work is not contributed by the Pt based materials, we have re-evaluated the HER activity of all CCE/MoS_x samples using graphite rod as an alternative counter electrode. As shown in **Figure S7**, the cathodic current densities were almost idential no matter Pt or C rod was used as counter electrode. Moreover, considering that faradaic efficiency of OER on Pt counter electrode is more than 95% during 6h of running HER, we believe that the presence of the Pt counter electrode did not cause altered electrochemical performance.

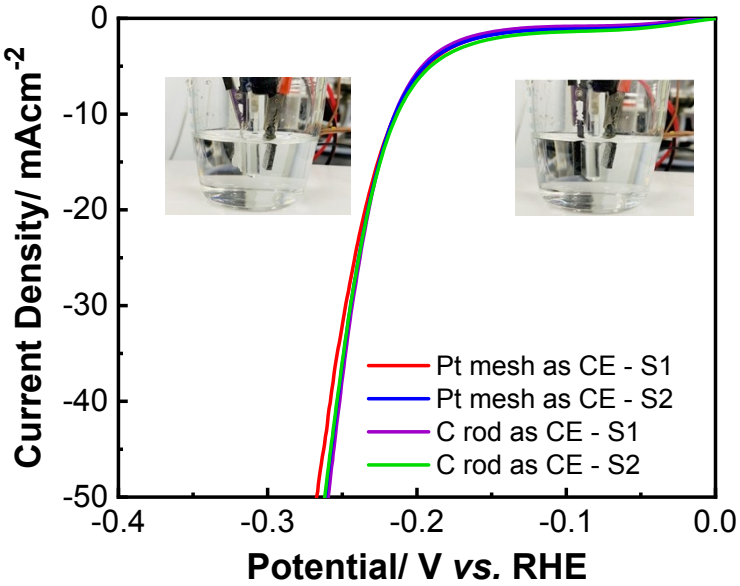

Figure S7 Current density (J) vs. potential (V) curve of HI-CCE/MoS_x (DMF: H_2O) in 0.5 M H_2SO_4 using Pt or graphite rod as counter electrode. Inset: Digital photograph of gas bubbles formed on the electrode surface during the test.

Table S2 Loading weight of MoS_x catalyst loaded on CCE substrates

Sample	Loading amount (mg/cm^2)
HO-CCE/MoS_x	1.23±0.08
HI-CCE/MoS_x	1.34±0.11
HI-CCE/MoS_x (DMF: H_2O)	1.53±0.14

To ensure a fair comparison, we have also normalized the performance of different electrodes (except for the blank CCE) by their corresponding actual catalyst loadings as shown in **Fig. S8** and found that the HI-CCE/MoS_x (DMF:H_2O) still shows the best performance among the samples.

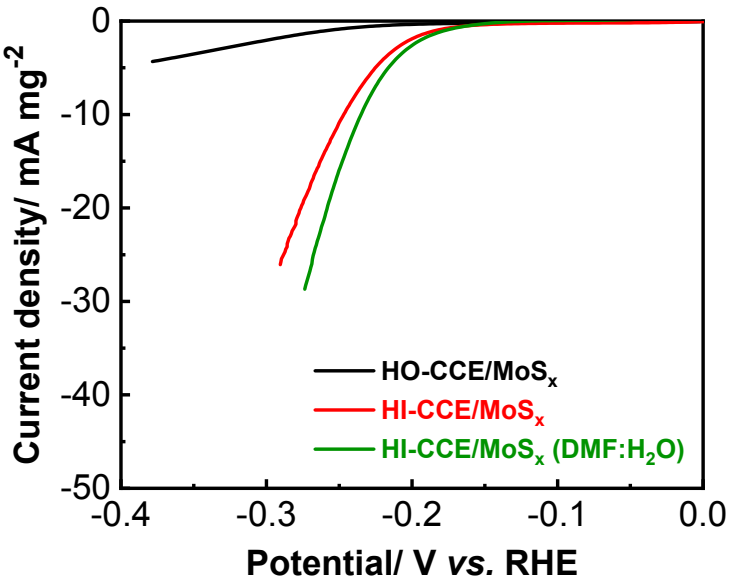

Figure S8 Polarization curves of the catalysts in 0.5 M H_2SO_4. The current densities are normalized by the mass loading.

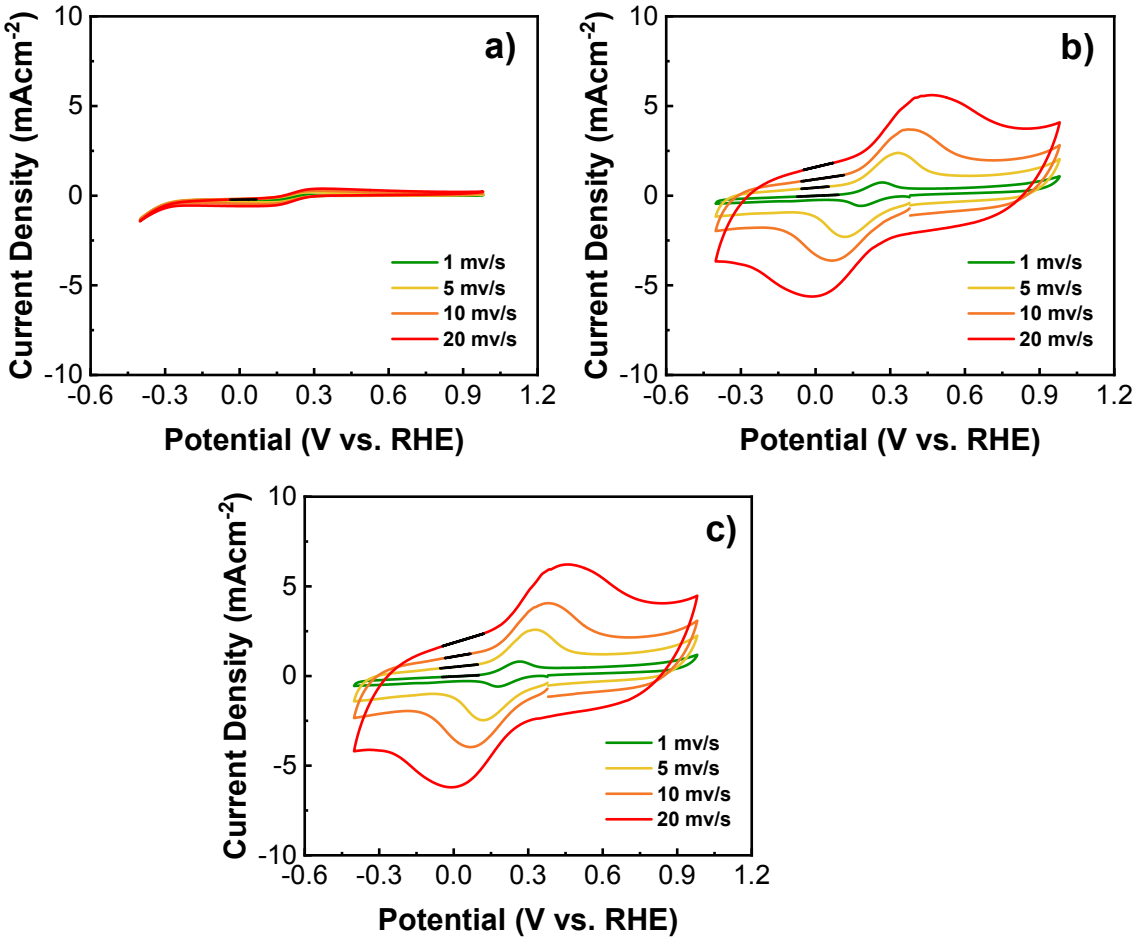

Figure S9 Cyclic voltammograms of HO-CCE/MoS_x (a, zoomed in inset) and HI-CCE/MoS_x (b) and HI-CCE/MoS_x (DMF: H_2O) at different potential scanning rates from 1 to 10 mVs^{-1}.

The turnover frequency (TOF), defined as the number of H_2 molecules evolved per active site per unit time, is an essential parameter to contrast the inherent catalytic activity of different systems. The TOF can be calculated from Faraday's law of electrolysis (assuming 100% Faradic efficiency using the expression[4–7]

$$\mathrm{TOF} = \frac{J.N_A}{2\mathrm{FN}}$$

The TOF is calculated using the current density (j) and the active site density (N) according to the following equation:

$$TOF = \frac{\text{Total number of } H_2 \text{molecules per second}}{\text{Total number active sites per unit area}} = \frac{\mathrm{J}}{2F\mathrm{N}}$$

Where J is the current density during hydrogen evolution in 0.5 M H_2SO_4, (mA/cm^2)

F is the Faraday constant, (96485 Cmol^{-1})

2 accounts for 2 electrons transfer per one H_2 molecule generation

N is the number of active sites

The active site density for the as-prepared samples was calculated using the relative roughness factor (R_f) of the catalysts according to references based on.

$$\mathrm{N_{sample}} = \mathrm{R_f} \times \mathrm{N_{flat\ standard}} = \frac{\mathrm{ECSA}}{\mathrm{Geometrical\ area}} \times \mathrm{N_{flat\ standard}}$$

From references[8,9], we know that the density of HER active sites in smooth planar MoS_2 surface is 1.164×10^{15} cm^{-2}. We chose to use a MoS_2 flat standard due to the difficulty of fabricating a perfectly flat, well-defined amorphous molybdenum sulfide catalyst[10]

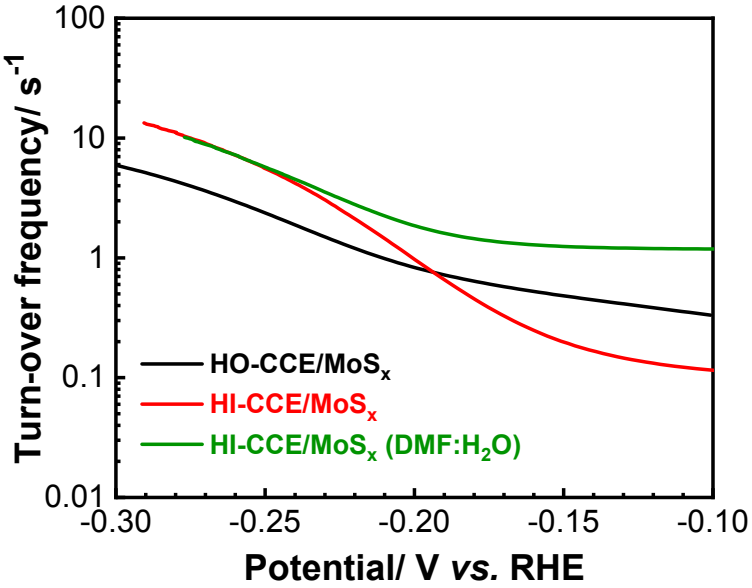

Figure S10 Evolution of the TOF with the applied potential of HO-CCE/MoS_x, HI-CCE/MoS_x and HI-CCE/MoS_x (DMF: H_2O).

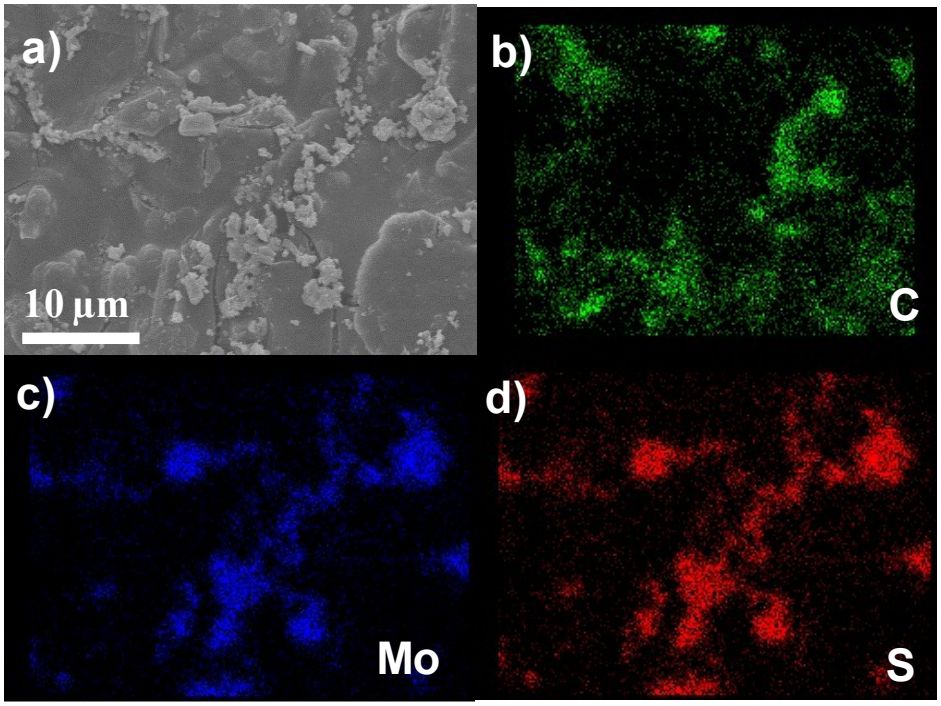

Figure S11 SEM images (a) and elemental mapping (b-d) for HI-CCE/MoS_x (DMF: H_2O) after HER

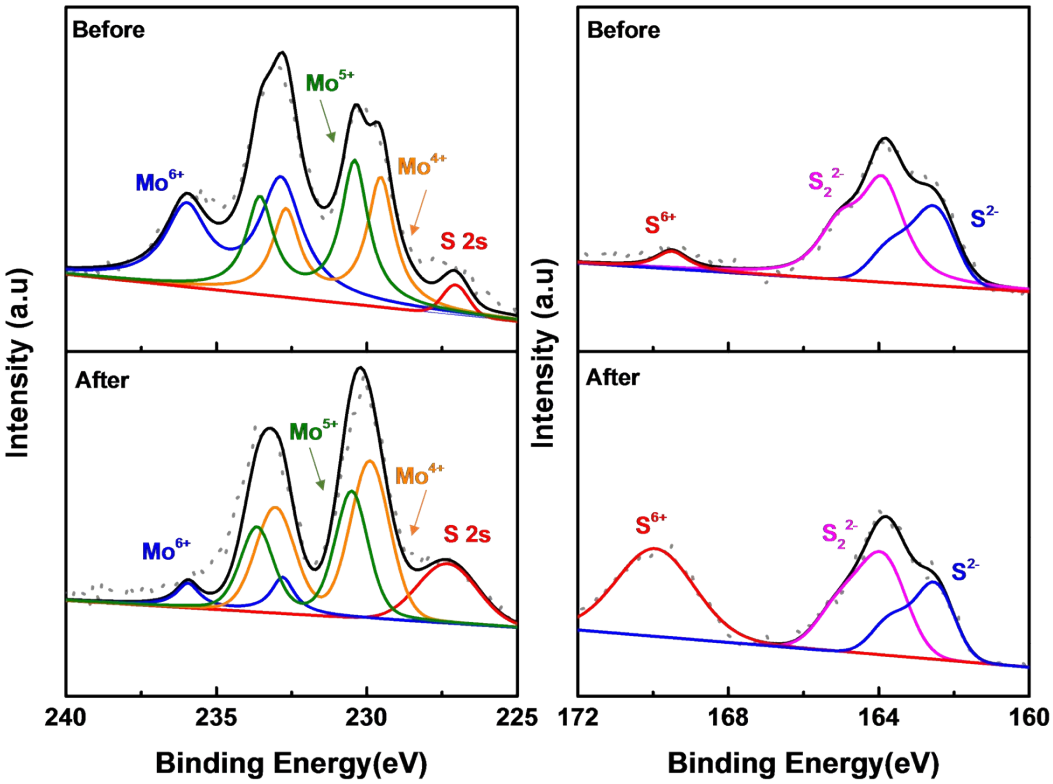

Figure S12 High-resolution XPS of HI-CCE/MoS_x (DMF: H_2O) before and after HER for 6h

REFERENCES

1 Y. Ohnuki, H. Matsuda, T. Ohsaka and N. Oyama, *J. Electroanal. Chem. Interfacial Electrochem.*, 1983, **158**, 55–67.

2 A. J. Bard and L. R. Faulkner, *Electrochemical Methods*, Wiley, New York, 2011.

3 T.-Y. Huang, C.-W. Kung, H.-Y. Wei, K. M. Boopathi, C.-W. Chu and K.-C. Ho, *J. Mater. Chem. A*, 2014, **2**, 7229–7237.

4 G. Zhao, K. Rui, S. X. Dou and W. Sun, *Adv. Funct. Mater.*, 2018, **28**, 1803291.

5 Y.-H. Choi, J. Lee, A. Parija, J. Cho, S. V Verkhoturov, M. Al-Hashimi, L. Fang and S. Banerjee, *ACS Catal.*, 2016, **6**, 6246–6254.

6 R. Bose, S. K. Balasingam, S. Shin, Z. Jin, D. H. Kwon, Y. Jun and Y.-S. Min, *Langmuir*, 2015, **31**, 5220–5227.

7 L. Li, Z. Qin, L. Ries, S. Hong, T. Michel, J. Yang, C. Salameh, M. Bechelany, P. Miele, D. Kaplan, M. Chhowalla and D. Voiry, *ACS Nano*, 2019, **13**, 6824–6834.

8 N. Huang, R. Peng, Y. Ding, S. Yan, G. Li, P. Sun, X. Sun, X. Liu and H. Yu, *J. Catal.*, 2019, **373**, 250–259.

9 S. Shin, Z. Jin, D. H. Kwon, R. Bose and Y.-S. Min, *Langmuir*, 2015, **31**, 1196–1202.

10 J. D. Benck, Z. Chen, L. Y. Kuritzky, A. J. Forman and T. F. Jaramillo, *ACS Catal.*, 2012, **2**, 1916–1923.